Journal of Alloys and Compounds, 195 (1993) 149–156
JALCOM 7436

X-ray texture analysis in YBaCuO ceramics and films

M. Pernet, D. Chateigner and P. Germi

Laboratoire de Cristallographie, CNRS, associé à l'Université J. Fourier BP 166, 38042 Grenoble Cedex 09, France

Abstract

The technological applications of high temperature superconductors will be possible only for bulk samples or thin films exibiting high critical current density. It has been confirmed that the superconducting properties of polycrystalline materials are strongly orientation-dependent, these properties being affected by the orientation of the crystallites. The simplest method to analyse the preferred orientation or "texture" of a crystalline material is to compare qualitatively the intensities of (*hkl*) reflexions of an X-ray diffraction pattern. This allows, however, only a rough estimation of the main features of the texture. Another method is the pole figure determination which gives the crystallographic orientation of the crystallites with respect to a specific orientation of the sample.
In YBaCuO samples, generally the (*00l*) pole figures define the c-axis alignment, while the (*hkl*) pole figures give information concerning the rotation about the c-axis i.e. the "in plane texture". The pole-figure technique allows one to compare different samples, to analyse the effects of processing parameters and to study epitaxial relationships. Texture analysis of YBaCuO oriented ceramics and uni and multi-layer films are presented.

1. Introduction

The technological applications of high temperature superconductors (HTS) will be possible only for bulk samples or thin films exibiting high critical current density. The conductivities of the cuprate superconductors being highly anisotropic, techniques for developing strong preferred orientations or "texture" in polycrystalline materials have been successful in improving critical current densities in many of these materials. In such materials the texture analysis describes statistically the orientation distribution of the crystallographic axis of the grains (crystallites) with respect to a set of macroscopic sample axes. When the texture is strong, most of the grains have almost identical orientations; whereas, when the texture is weak, the grain orientations are almost random.
Most texture assessments of HTS ceramics are based on a qualitative visualization of morphology, on indirect determination of properties or on estimates from X-ray powder patterns. Preferred orientation of thin films has been traditionally assessed by peak ratios of diffraction peaks measured with an X-ray powder diffractometer. All these methods allow only a rough estimation of the main features of the texture. Another method, pole figure determination, gives the crystallographic orientation of the crystallites with respect to a specific orientation of the sample. Additionally this method allows one to compare different samples, to analyse the effects of processing parameters and to study epitaxial relationships. Texture analysis of oriented ceramics and films are presented.

2. Experimental

X-ray pole figures were obtained using the Schulz reflection technique [1]. A schematic of the geometry is shown in Figure 1. The method requires a special specimen holder. The intensity is measured by fixing the Bragg angle θ and rotating the sample successively around the axis normal to the surface (azimuthal angle β) and around a horizontal axis (tilt angle φ) which lies on the specimen surface. The intensity is proportional to the volume fraction of crystallites having the normal to the (*hkl*) plane bissecting the angle between the incident and the diffracted beams. For a recent overview of standard experimental techniques and methods of texture analysis see Ref. [2].

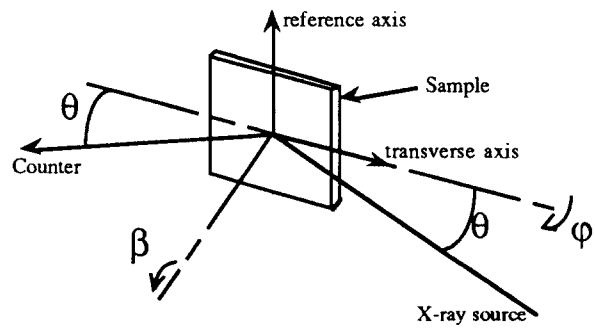

Figure 1. The Schulz geometry used in the X-ray pole-figure analysis

0925-8388/93/$06.00

The tilt rotation measured by the angle φ, can be varied from 0° to 90°, while the normal rotation, versus an angle β, can be simultaneously taken from 0° to 360°. The studies where made by using a GMI-Dosophatex pole figure goniometer with a Ni-filtered Cu radiation. In our experiments the φ angles where usually set at preselected values, at which the β scans where made from 0° to 360°. So a map of the orientations of the normals to the (*hkl*) planes of the crystallites-a pole figure-is obtained. A random powder sample analysis is run on the peak corresponding to the same set of (*hkl*) reflexions to correct the data for defocusing, absorption and geometrical effects. Finally, a pole figure is plotted from the corrected data on a polar stereographic projection (Figure 2). Iso-intensity lines indicate the relative intensity of the pole related to the maximum diffracted intensity. In general a single (*hkl*) pole figure does not give the full information about the texture of the material. However, by combining the data of at least two (*hkl*) pole figures, the complete three dimensional orientation distribution can be estimated.

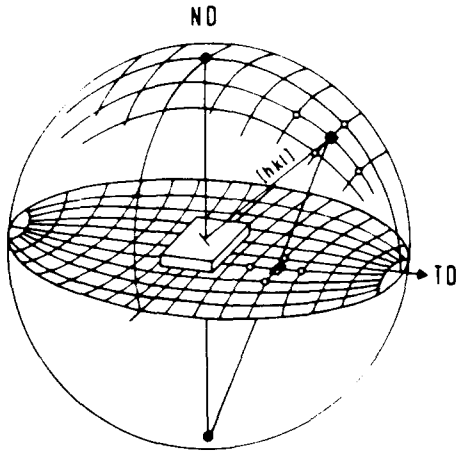

Figure 2. Stereographic projection of (*hkl*) pole.

In the case of 123 YBaCuO samples the (*00l*) pole figures define the c-axis alignment while the (*hkl*) pole figures give information concerning the rotation about the c-axis, i. e. the in-plane texture. By using the X-ray pole figure method we can analyse the texture of an area of the order of 1 mm^2 with about 10 μm of depth.

3. Results and discussion

3.1. Defocalization correction

In the Schulz reflection method a progressive broadening of the reflected beam occurs due to the tilting of the sample. This effect may give rise to a loss of intensity if the reflected beam becomes broader than the aperture slit of the counter. The study of the attenuation of the measured intensity due to the defocussing effect has lead to the publication of analytical correction formulae depending of the kind of samples, bulk [3-5] or film [6].

3.2 Texture analysis in ceramics

Texture in bulk ceramic superconductors can be achieved by different methods, such as magnetic alignment of powder particles, directional solidification and others. Some of them show a strong effect on texturing, some show a weak effect. Using the pole figures technique, the textures achieved by different methods can be compared.

Magnetically aligned materials

In $YBa_2Cu_3O_7$ type materials the grain alignment process in the magnetic field relies on the anisotropy between the c-axis magnetic susceptibility and the basal-plane susceptibility. Pole figures of a magnetically oriented YBaCuO ceramic prepared from a liquid suspension of single crystals [7] are shown in Figure 3. This "multipoles figure" represents the distribution of two kinds of poles : (007) and (103).

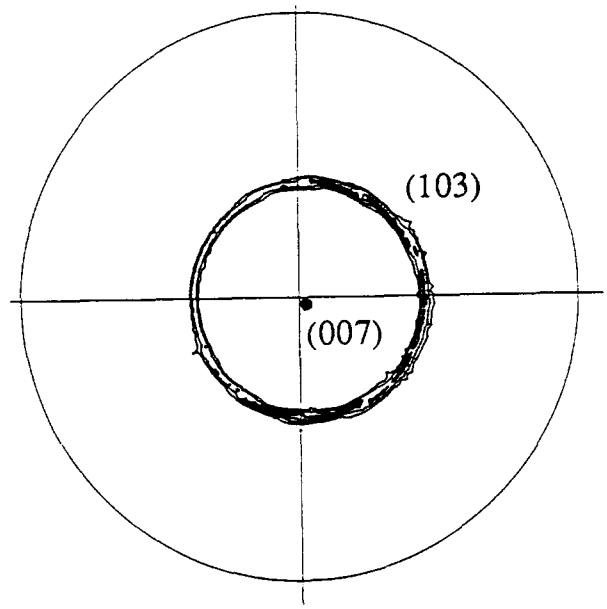

Figure 3. "Multipoles figure" showing the (007) and (103) poles of a magnetically oriented YBaCuO sample.

The (007) pole figure defines the c-axis alignment; the localization of these poles within a small area indicates that the crystallites are strongly aligned with their c axes parallel to the magnetic field. The (103) poles are localized on a ring corresponding to a ϕ angle of 45°, which is the calculated value of the angle between the [007] and [103] directions. Taken together, these results allow us to conclude that the sample exibits a fibrous texture in which the fibre axis coincides with the

direction of the applied magnetic field (perpendicular to the surface sample).

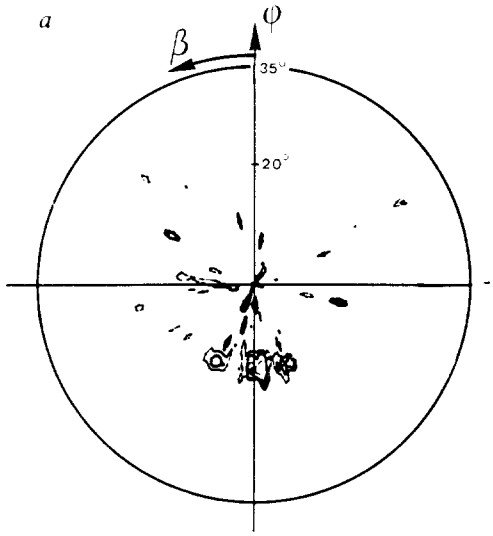

Figure 4. (007) pole figure measured on a surface cut perpendicular to the magnetic field.

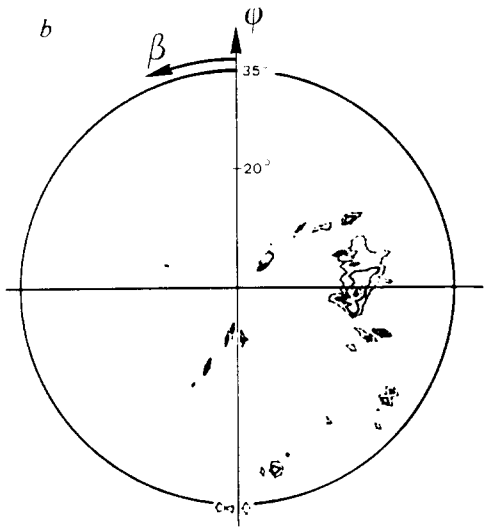

Figure 5. (200) pole figure measured on a surface cut parallel to the magnetic field.

A bulk textured sample may be produced by application of a magnetic field during the solidification of the compound via peritectic phase transformation [8]. Figures 4 and 5 show pole figures for two orthogonal directions with β ranging from 0° to 360° and ϕ ranging from 0° to 35° with a step of 1.8°.The (007) pole figure was measured by diffraction on a surface cut perpendicular to the field. No pole appears for ϕ>35°. This figure defines the c-axis alignement which coincides with the direction of the applied field and lies about 15° from the normal to the projection plane. By diffraction on a surface cut parallel to the field, the (007) poles are extremely weak whereas the (200) poles are localized within a small area. So the a-axis direction makes an angle of about 20° with the normal to that surface. The pictures of the two surfaces remain coherent. We can conclude that the observed texture is a bulk and not a surface property.

Melt textured materials

Efficient texturation is obtained by crystallisation from a liquid. The Melt Textured Growth process (MTG) is particularly attractive [9]. This involves bringing the initial 123 YBaCuO sintered sample to high temperature and then cooling it slowly under a thermal gradient to obtain a directional solidification. Nevertheless texturation experiments have been carried out without thermal gradient. In these cases, the cooling rate plays an essential part in the crystallization and the texturation.

Figure 6 shows the pole figures for an oriented ceramic obtained by using a zone melting process [10]. The (007) pole indicates that the [*00l*] directions of the crystallites make an angle of about 8° with the normal to the surface of the sample and are dispersed along a cone portion of about 20° in β. The (013) poles show a four-fold symmetry as a clear evidence of twinning. In an orthogonal direction related to the previous surface the (200) poles (not shown here) are localized within a small area. Consequently the a-axis direction (or b-axis because of twinning) coincides with that direction. As the pictures of the two studied surfaces are coherent we can conclude that the zone melting process leads to a tri-dimensional texture.

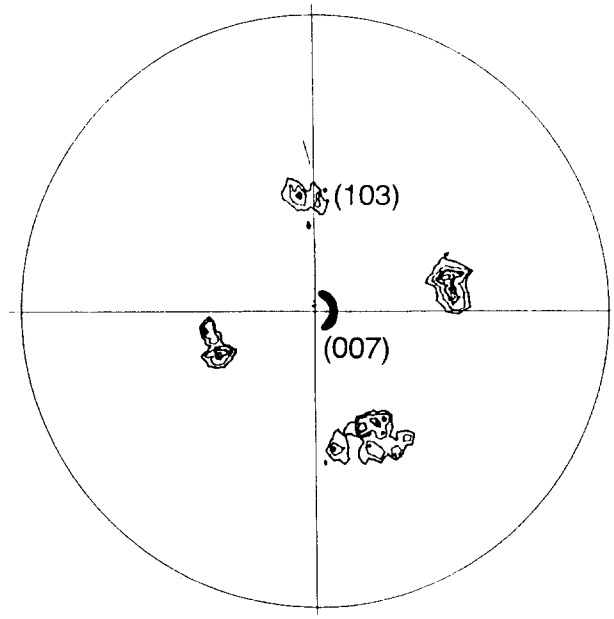

Figure 6. The (007) and (013) pole figures of a ceramic textured by a zone melting process.

We analysed the texture of a ceramic obtained by a rather original method : the texture is realized in an horizontal furnace, on Y_2O_3 substrate, but without any external gradient [11]. Figure 7 presents the results for (007), (103) and (113) poles from a first surface (a) and Figure 8. the (005) and (103) poles from a second surface (b) perpendicular to the previous one. It indicates that the *[00l]* directions of the crystallites make an angle of about 10° with the normal to the surface (b) of the sample. The (103) and (113) poles show a four-fold symmetry as a clear evidence for twinning.

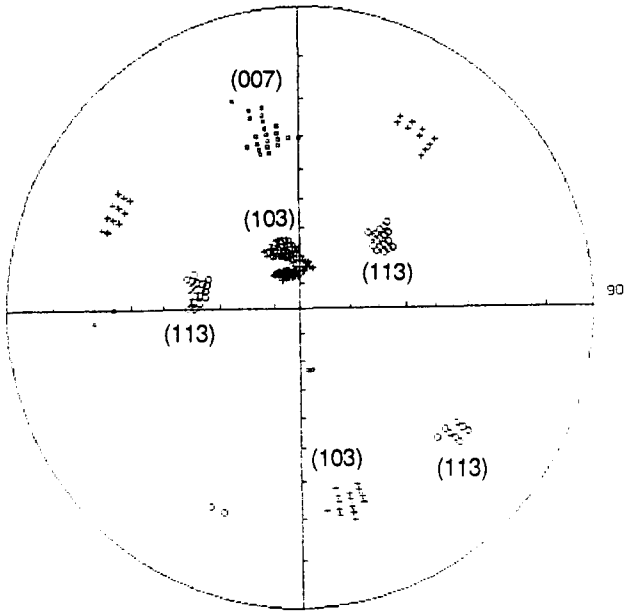

Figure 7. (007), (103) and (113) pole figures from surface (a) of a melted textured ceramic on Y_2O_3 substrate.

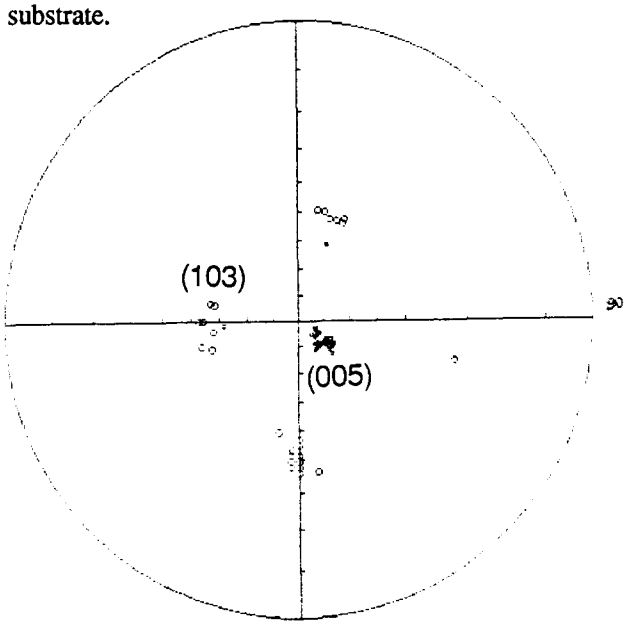

Figure 8. (005) and (103) pole figures from surface (b).

In the case of 123 YBaCuO, the unit cell parameters have the relationship of a≈b≈c/3. Therefore the [103] direction which can be considered as [101] in the cubic system makes an angle of about 20° with the normal to the surface (a). The pole figures drawn on two perpendicular surfaces show that the texturation is present throughout the bulk.

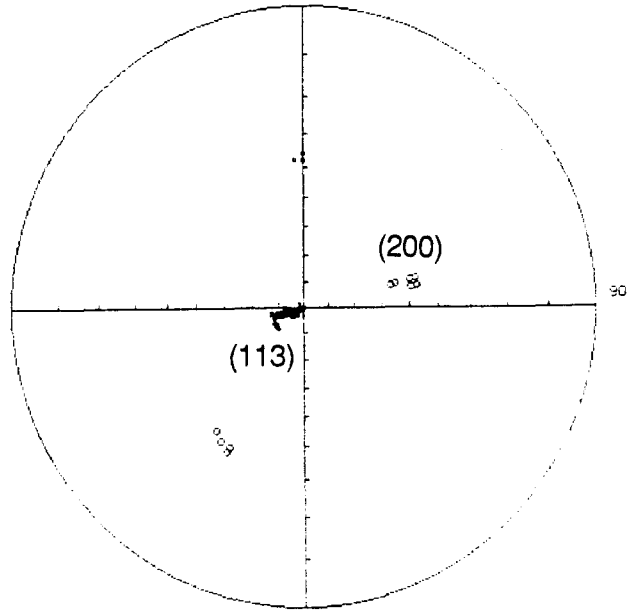

Figure 9 (a). (113) and (200) pole figures from face (a) of a melt textured ceramic.

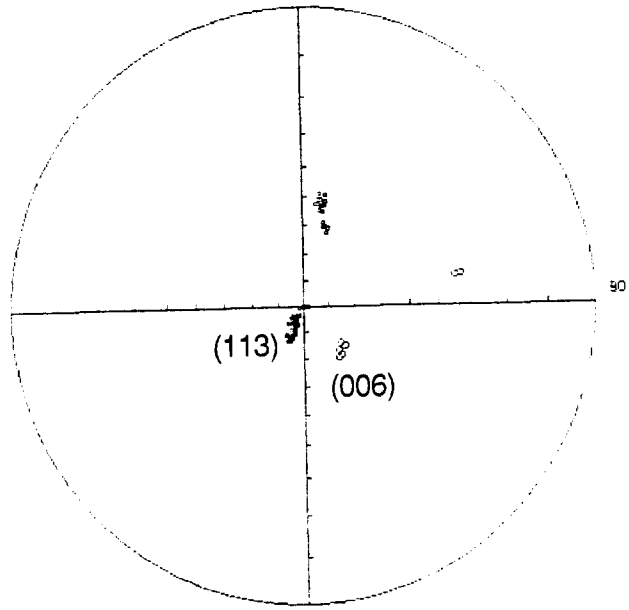

Figure 9 (b). (113) and (006) pole figures from face (b) perpendicular to the face (a).

In certain conditions the melt textured process gives rise to a surface texture. Pole figure measurements have

shown that the preferential orientation of the free surfaces of a bulk sample remains unchanged : direction [113] whatever the face of the considered parallelepiped (Figure 9.) This observation is in agreement with the existence of misoriented regions inside the sample [12].

Bulk textured by the diffusion couples technique

The $YBa_2Cu_3O_{7-\delta}$ superconducting phase has been synthezied from the diffusion couples Y_2BaCuO_5-$BaCuO_2$ [13]. A three-dimensionnal texture has been obtained similar to that resulting of the zone melting process (Figure 10).

Texture analysis by neutron diffraction

In the near future neutrons will be employed for pole figure measurements in a well textured ceramic. The main reason is that neutrons are about 1000 times more penetrating than X-rays in such materials. This means than in neutron diffraction the analysed depth can be in the "cm" range (in the transmission case) whereas in the X-ray Schulz technique it is in the "μm" range. Hence, the advantage of neutron diffraction is that bulk textures rather than surface textures are studied.

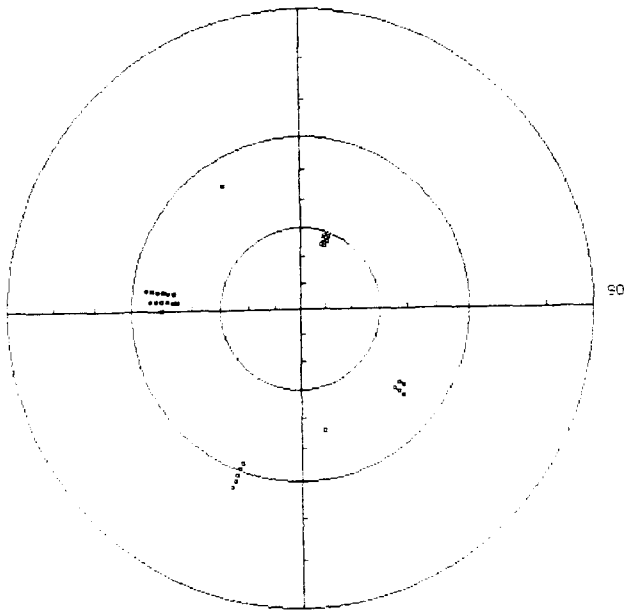

Figure 10. (103) pole figure from a sample produced by the diffusion couples technique.

3.3 Texture analysis in films

Study of the texture of YBaCuO thin films is important to understand other superconductive parameters than critical current density such as microwave resistivity, Josephson junction.... Usually X-ray diffraction measurements in the Bragg mode showing only (*00l*) reflections indicate c-axis oriented films. Elsewhere the mosaic spread may be determined from the width of corresponding rocking curves. The X-ray pole-figure analysis method is not only an effective way to study the texture of YBaCuO films, but an excellent way to quantify the lattice alignments between the film and the substrate provided the film is thin enough for X-rays to penetrate and to be diffracted by the substrate lattice.

Since numerous kind of substrates have been involved for films growth (MgO, $SrTiO_3$, Al_2O_3, $LaAlO_3$ ...) and that number of different technics (Laser ablation, magnetron sputtering, MOCVD ...) have been used for their elaboration, we present here only characteristic examples of well textured samples, i.e. up to now on single crystal substrates and deposited by laser ablation methods. For the texture analysis of films we reveal the existence of the in-plane preferred orientation by the complex (103/013) pole, since there is a lot of (110) twinning in the samples. Due to the strong texture, there is only one ring of interest on the (103) pole figure, and consequently the analysed zone was $42.75° \leq \varphi \leq 47.25°$ limited by the two circles on the figures. Accordingly, the scanning steps $\Delta\varphi$ and $\Delta\beta$ can be reduced as less as 0.225°.

We use for the description of texture components the general formulation : $\mathbf{x}_{\perp\alpha}$ where **x** is the lattice parameter of the film (here **a**, **b** or **c**) perpendicular to the substrate surface revealed by classical θ-2θ scanning, and α the angle between the in-plane lattice parameter of the film relatively to the substrate ones. In our pole figures, α is measured by the azimuthal angle β value. From that $\mathbf{x}_{\perp\beta}$ texture is deduced the epitaxial mismatch which induce stress fields in the layer [14].

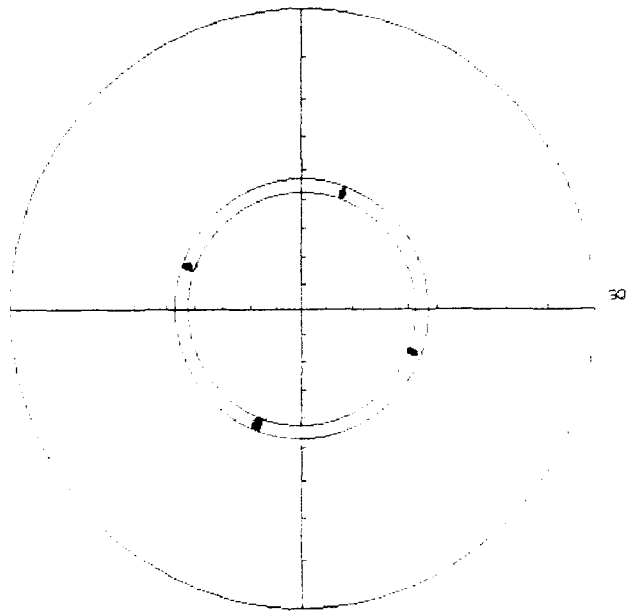

Figure 11. (103) pole figure of a (*00l*) oriented film on $SrTiO_3$ single crystal substrate.

The mismatch due to epitaxy will be calculated here by $|d_s-d_f|/d_f$ where d_s is the principal interplanar distance of the substrate in the plane of deposition (for which $\beta=0$) and d_f the one of the film superposed to d_s.

Film on $SrTiO_3$-(100) single crystal

The unit cell parameter of $SrTiO_3$ (3.905Å) displays a low mismatch (≈2%) with the YBaCuO superconducting phase, resulting in highly textured films. Fig.11 shows an example of such films where is only present the principal $c_{\perp 0}$ texture component. The width of the poles corresponds both to the (110)-twinning effect due to the orthorhombicity of the film, therefore its oxygen contents [15], and on texture sharpness. In this case we notice a rather weak width (≈1.5° at I=15% of the maximum intensity).
The (111)-substrate pole figure was also done which shows signals at $\beta=45°$ from the (103)-YBCO poles as a confirmation of the $c_{\perp 0}$ orientation.

Films on MgO-(100) single crystal

MgO is also widely used for YBCO epitaxy particularly in view to the elaboration of hyperfrequency devices. Its unit cell parameter (4.213Å) gives a relatively large lattice mismatch (≈10%) which however does not prevent YBCO films with strong texture. Fig.12 shows clearly that a good $c_{\perp 0}$ epitaxial growth of YBCO can be obtained on 1500Å thick films. The poles have a width of 4° approx. at I=15%.

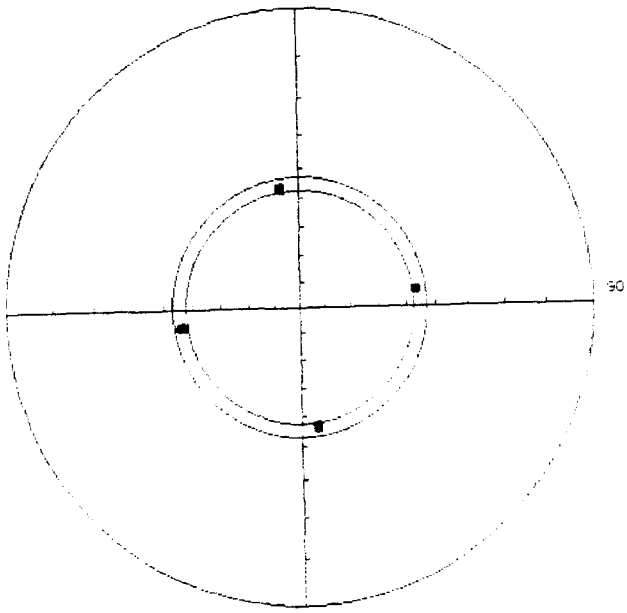

Figure 12. (103) pole figure of a (*00l*) oriented film on MgO single crystal substrate.

Nevertheless, the weak intensity details are not observable on this figure since they are less than a few percent. Fig.13 is a pseudo-3D representation of the same pole figure. The data were analysed from different cross sections along the periphery of circles at constant φ values, and are developped in successive β-scans. A second texture component, $c_{\perp 45}$, is visible in the range 1-2% of the principal one. A critical current density of 5.10^5 A/cm^2 was measured on this sample.

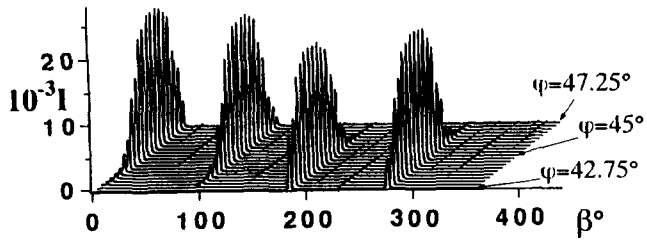

Figure 13. Pseudo-3D representation of figure 12. This sample exhibits a Jc of 5.10^5 A/cm^2.

The other orientations $c_{\perp 18}$ and $c_{\perp 26}$ are not completely understood, they seem to be a combination of a substrate diffraction effect via white spectrum of Cu cathode emission and coincidence site lattice misorientations in the layer itself. These points are under investigations.

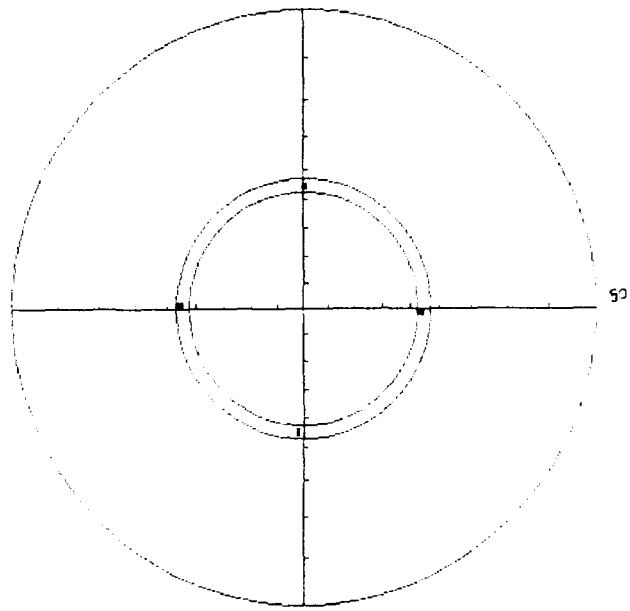

Figure 14. (220)-pole figure of a MgO substrate used for films growth.

Fig.14 shows the (220)-pole figure of the precedent sample substrate. The poles are very narrow (≈1° at I=15% including the experimental width) like it was expected for a single crystal. They are located at the same β position as (103)-YBCO poles, indicating the $c_{\perp 0}$ texture of the film. A comparison has to be made with the larger poles width of the film, to underline the non single crystalline character of the latter.
A similar, but less carrier capable, sample (Jc=3.10^4 A/cm^2) has been analysed (fig.15) which shows $c_{\perp 45}$ orientation of greater importance (6-7%). This fact confirmed the drastic decreasing effect of highly misoriented grains on Jc [16, 17].

Bi-layer of YBCO/YSZ on Al_2O_3-(1$\bar{1}$02) single crystal
The need to avoid Al diffusion into the YBCO film leads to an intercalation of a buffer layer, which also has to provide good matching. The choice of the cubic cell phase (5.139Å) $Y_xZr_{(1-x)}O_{2-\delta}$ (YSZ:x=0.15) achieves this combination. A 3000Å-YBCO and 600Å-YSZ sample was analysed and results are presented on fig.16. The (103)-YBCO and (111)-YSZ poles are aligned at the same β as an evidence of $c_{\perp 45}$ principal texture between the two layers. This epitaxial relation is favoured from an energy point of view since it leads to a lower lattice mismatch than a $c_{\perp 0}$ configuration (≈5% and ≈34% for $c_{\perp 45}$ and $c_{\perp 0}$ respectively).

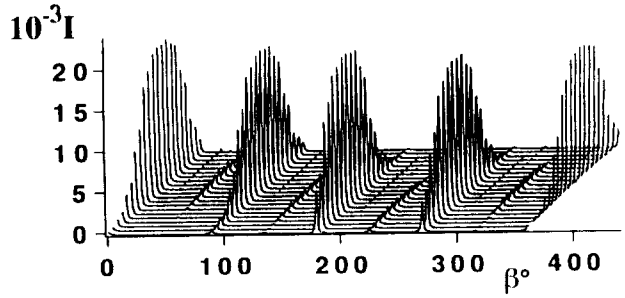

Figure 15. (103) pole figure of a low Jc (3.10^4 A/cm^2) YBCO/MgO sample.

The measured width at I=15% of (103)-YBCO and (111)-YSZ poles are respectively of 4.3° and 2.9°. This provides evidence of the buffer function of YSZ layer.

YBCO/$La_2CuO_{4-\delta}$ multilayer/MgO-(100) substrate
A six times YBCO/LCO unit was deposited, the total thickness being of the order of 1000Å. The same reasoning as in the preceding case can be proposed since the lattice parameters of the orthorhombic LCO basal plane (5.36Å and 5.40Å) are close to that of YSZ, leading to a ≈9% mismatch factor. Therefore, the $c_{\perp 45}$ texture is expected between YBCO and LCO. This principal component is confirmed by the analysis of (103)-YBCO and (113)-LCO pole figures on fig.17.

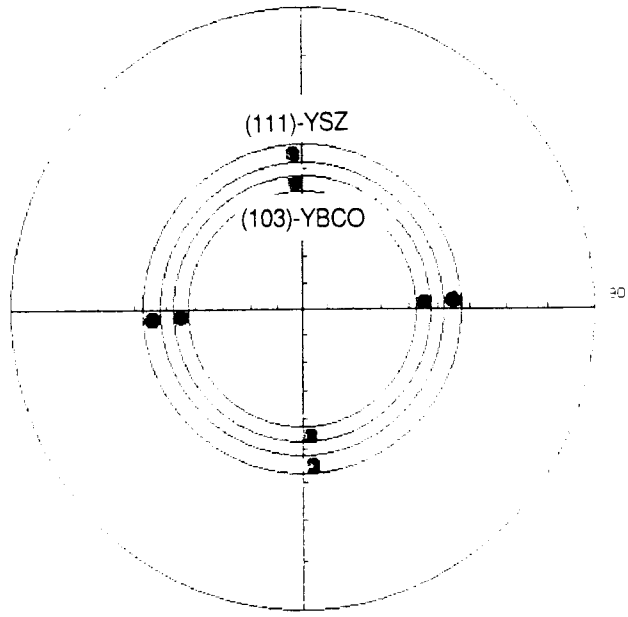

Figure 16. (103)-YBCO and (111)-YSZ multipole figure of a YBCO/YSZ/Al_2O_3 bilayer.

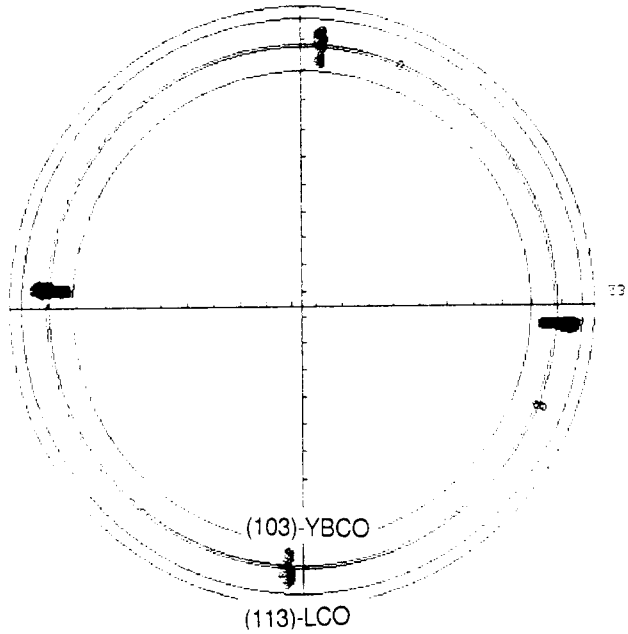

Figure 17. (103)-YBCO and (113)-LCO multipole figure of a YBCO/LCO multilayer on MgO.

The epitaxy of all the layers is forced by the first deposited LCO layer, which is $c_{\perp 45}$ relatively to MgO,

and which correspond to a lightly lower strain mismatch than an hypothetic $c_{\perp 0}$ (16% for only 18% respectively). However this slight difference may allow the $c_{\perp 0}$ texture.

The breadth of the LCO poles are larger than those of YBCO. Since the lattice orthorhombicity factor (a-b)/b is less important in LCO, we can conclude in this case that a better texturation is obtained in YBCO.

4. Conclusion

The pole figure technique is an effective way to determine the texture of YBCO oriented ceramics and films and provides more information than classical Bragg diffraction scans or rocking curves. The texture of a number of samples can be analysed to be correlated with preparation techniques and physical properties.

Acknowledgments

The authors express their thanks to the Alcatel-Alsthom Recherche Laboratories (Marcoussis), the LETI (Grenoble), the CRTBT (Grenoble), the CRPHT (Orléans), the LCS (Bordeaux) and the Institute of Physics of Solid (Minsk) for providing the different samples.

One of them (D.C.) gratefully acknowledges the support of Alcatel-Alsthom Recherche for his doctoral study.

References

1 L.G. Schulz, J. Appl. Phys., 20 (1949) 1030.
2 H.J. Bunge (ed.), Experimental techniques of texture analysis, DGM Oberursel, 1986.
3 J.R. Holland, Advanc. X-ray Anal., 7 (1964) 86.
4 E. Tenckhoff, J. Appl. Phys., 41 (1970) 3944.
5 E.M. Huijser-Gerits and G.D. Rieck, J. Appl. Cryst.,7 (1974) 286.
6 D. Chateigner, P. Germi and M. Pernet, J. Appl. Cryst., 25 (1992)
7 M. Lees, P. de Rango, B. Giordanengo, T. Fournier, P. Lejay and R. Tournier, Proc. ICMAS 90, R. Tournier and R. Suryanarayanan (eds.) IITT International (1990) 49.
8 P. de Rango, M. Lees, P. Lejay, A. Sulpice, R. Tournier, M. Ingold, P. Germi and M. Pernet, Nature, 349 (1991) 770.
9 S. Jin, T.H. Tiefel, R.C. Sherwood, M. E. Davis, R.B. van Dober, G.W. Kammott, R.A. Fastnacht, H.D. Keith, Appl. Phys. Lett., 52 (1988) 2074.
10 A. Wicker, Journées SEE (Caen 1990 France)
11 N. Pellerin, P. Simon, P. Odier, D. Chateigner, P. Germi, M. Pernet and J.P. Bonnet, Proc. ICMAS 92, C.W. Chu and J. Fink (eds) IITT International, Gournay sur Marne France
12 J.M. Heintz, C. Magro, P. Dordor, J.P. Bonnet, D. Chateigner, P. Germi, M. Pernet, D. Machajdik and A. Pevela, Proc. Critical Currents in High Tc Super conductors (Vienne 1992) to appear in Cryogenics
13 V.V. Pankov, T. Fournier, M. Pernet, V.N. Shambalev and N.A. Kalanda, to appear in Mat. Res Bull.
14 A. Segmüller, I.C. Noyan & V.S. Speriosu, Prog. Crystal Growth and Charact., 18 (1989) 21-66.
15 D. Chateigner, P. Germi and M. Pernet : to be published.
16 D. Dimos, P. Chaudhari, J. Mannhart & F.K. LeGoues, Phys. Rev. Lett., 61 (1988) 219-222.
17 M.F. Chisholm & S.J. Pennycook, Nature, 351 (1991) 47-49.